Intracellular routing of β-catenin

Hendriksen, J.V.R.B.

CHAPTER 2

RanBP3 enhances nuclear export of active ß-catenin independently of CRM1

JCB, Vol. 171, No. 5, p 785-797 December 5, 2005

RanBP3 enhances nuclear export of active ß-catenin independently of CRM1

Jolita Hendriksen[1], Francois Fagotto[2], Hella van der Velde[1], Martijn van Schie[3], Jasprien Noordermeer[3], and Maarten Fornerod[1]

1 Department of Tumor Biology, Netherlands Cancer Institute, 1066 CX Amsterdam, Netherlands
2 Department of Biology, McGill University, Montreal, Quebec, Canada H3A 2T5
3 Department of Molecular Cell Biology, Leiden University Medical Center, 2333 AL Leiden, Netherlands

ß-Catenin is the nuclear effector of the Wnt signaling cascade. The mechanism by which nuclear activity of ß-catenin is regulated is not well defined. Therefore, we used the nuclear marker RanGTP to screen for novel nuclear ß-catenin binding proteins. We identified a cofactor of chromosome region maintenance 1 (CRM1)–mediated nuclear export, Ran binding protein 3 (RanBP3), as a novel ß-catenin–interacting protein that binds directly to ß-catenin in a RanGTP-stimulated manner. RanBP3 inhibits ß-catenin–mediated transcriptional activation in both Wnt1- and ß-catenin–stimulated human cells. In X. laevis embryos, RanBP3 interferes with ß-catenin–induced dorsoventral axis formation. Furthermore, RanBP3 depletion stimulates the Wnt pathway in both human cells and D. melanogaster embryos. In human cells, this is accompanied by an increase of dephosphorylated ß-catenin in the nucleus. Conversely, overexpression of RanBP3 leads to a shift of active ß-catenin toward the cytoplasm. Modulation of ß-catenin activity and localization by RanBP3 is independent of adenomatous polyposis coli protein and CRM1. We conclude that RanBP3 is a direct export enhancer for ß-catenin, independent of its role as a CRM1-associated nuclear export cofactor.

The Wnt signaling pathway regulates a variety of processes during homeostasis and development, including cellular proliferation, cell fate decision, axis formation, and organ development (Nusse, 1999). Deregulation of the pathway is implicated in many human cancers (Polakis, 2000). The key effector protein of the Wnt pathway is the transcriptional activator ß-catenin. Cytoplasmic ß-catenin is efficiently trapped in a multiprotein complex containing adenomatous polyposis coli (APC; Groden et al., 1991; Kinzler et al., 1991), Axin (Zeng et al., 1997; Behrens et al., 1998), and glycogen synthase kinase 3ß (GSK3ß; He et al., 1995). In the absence of a Wnt signal, this complex rapidly phosphorylates ß-catenin, targeting it for degradation (Hart et al., 1998; Ikeda et al., 1998; Itoh et al., 1998; Sakanaka et al., 1998). Wnt binding to the Frizzled/LRP (low-density lipoprotein receptor–related protein) receptors results in inhibition of the APC–Axin–GSK3ß complex by activation of Dishevelled (Boutros and Mlodzik, 1999; Wharton, 2003) and by recruitment of Axin to the plasma membrane by LRP (Mao et al., 2001; Tolwinski et al., 2003). This results in an increase in nonphosphorylated ß-catenin that forms active transcriptional complexes in the nucleus with T cell factor (TCF)/lymphocyte enhancer binding factor (LEF) transcription factors (Behrens et al., 1996; Molenaar et al., 1996; Staal et al., 2002).

Nuclear activity of ß-catenin is regulated by several mechanisms. In the absence of a Wnt signal, TCF proteins occupy and repress promoters of their target genes by recruiting repressor proteins like Groucho, CtBP (COOH-terminal binding protein), and histone deacetylases (Cavallo et al., 1998; Levanon et al., 1998; Roose et al., 1998; Waltzer and Bienz, 1998; Brannon et al., 1999; Chen et al., 1999). Interaction of ß-catenin with TCF/LEF transcription factors results in activation of these genes. BCL-9/Legless and Pygopus have been shown to be essential components of the ß-catenin–TCF transcription complexes (Kramps et al., 2002; Parker et al., 2002; Thompson et al., 2002). ß-Catenin also interacts with chromatin remodeling and histone modification proteins such as Brg1 (Brahma-related gene 1) and CBP (CREB binding protein)/p300 to promote target gene activation (Hecht and Kemler, 2000; Takemaru and Moon, 2000; Barker et al., 2001). Furthermore, ICAT (inhibitor of ß-catenin and TCF4) and Chibby are identified as nuclear proteins that repress Wnt signaling by compet-

ing with TCF for binding to ß-catenin (Tago et al., 2000; Takemaru et al., 2003).
In this study, we aimed to identify new modulators of ß-catenin in the nucleus. We used the nuclear marker RanGTP to select for nuclear factors that directly bind ß-catenin and identified Ran binding protein 3 (RanBP3). We show that RanBP3 inhibits ß-catenin–TCF4–mediated transactivation in human cell lines by relocalization of active ß-catenin from the nucleus to the cytoplasm. In addition, we show that RanBP3 causes ventralization and inhibits ß-catenin–induced double axis formation in *X. laevis* embryos. Loss of *D. melanogaster* RanBP3 results in cuticle defects and expands the Engrailed protein expression domain. We conclude that RanBP3 functions as a novel type of inhibitor of ß-catenin and identify its gene as a candidate human tumor suppressor in the commonly deleted chromosomal region 19p13.3.

Results

RanBP3 interacts directly with ß-catenin in a RanGTP-stimulated way

To study the interaction between ß-catenin and nuclear transport factors, we used GST-tagged ß-catenin to pull down interacting proteins from X. laevis egg extracts. Interacting proteins were initially analyzed by Western blot using mAb414, which recognizes a phenylalanine glycine (FG)–rich epitope present in multiple nucleoporins. FG repeat–containing nucleoporins Nup62, Nup153, and Nup358 were specifically bound by full-length ß-catenin and by the central armadillo (ARM) repeat region (Chapter 5, Fig 5). Interestingly, we found a strong interaction between ß-catenin and two unknown proteins of ~80 and 90 kD that were recognized by mAb414 (Fig. 1 A, lanes 3 and 4). These proteins interacted with full-length ß-catenin and to a lesser extent with the ARM repeats (ARM 1–12). The mAb414 reactivity indicated that these two proteins contained FG repeats. Two isoforms of RanBP3 stood out as possible candidates for these two unknown proteins because they contain FG repeats and have the correct sizes. Indeed, recombinant human RanBP3-a comigrated with the p90 protein and was recognized by mAb414 (Fig. 1 A, lane 5). To confirm that RanBP3 was one of these new ß-catenin–interacting proteins, we repeated the pull-down experiment using HeLa nuclear extracts and an mAb recognizing human RanBP3. The b isoform of RanBP3 was more abundant in HeLa nuclear extracts and copurified with GST-tagged full-length and the ARM repeats of ß-catenin (Fig. 1 B). To mimic nuclear conditions, 2 µM of a nonhydrolysable mutant of the small GTPase Ran (RanQ69L-GTP) was added, resulting in increased interaction between ß-catenin and RanBP3 (Fig. 1 B, lanes 2 and 4). In the presence of RanQ69L-GTP, the less abundant a isoform of human RanBP3 also bound to full-length ß-catenin (Fig. 1 B, lane 2).
To investigate whether the binding between ß-catenin and RanBP3 was direct, we performed pull down assays with GST-tagged ß-catenin and recombinant RanBP3. Human RanBP3-b interacted directly with GST-ß-catenin with an optimum at 0.5 µM RanBP3 (Fig. 1C, lane 3). These binding characteristics resemble the interaction of RanBP3 with CRM1, which shows optimal binding at 0.2 µM RanBP3 (Englmeier et al., 2001). Furthermore, we used a RanBP3 mutant that cannot bind to RanGTP due to a point mutation in its RanGTP binding domain (RanBP3 "wv" mutant (Englmeier et al., 2001). This mutant interacted only very weakly with ß-catenin and lost its ability to bind at an optimum concentration (Fig. 1C, lanes 5-7). These data suggest that RanGTP increases the affinity of RanBP3 for ß-catenin. To confirm the RanGTP dependency, RanBP3 was bound to ß-catenin columns at the optimal concentration of 0.5 µM in the presence of RanGTP and eluted either in the absence or presence of the recombinant Ran cofactors RanBP1 and RanGAP (lanes 8-11). While virtually no RanBP3 was eluted with buffer only, significant amounts were detected after elution in the presence of either 0.5 µM RanBP1, 0.2 µM RanGAP or a combination of these.

RanBP3 inhibits transcription of a TCF responsive reporter

Wnt signaling ultimately results in the stabilization of ß-catenin that forms active transcriptional regulation complexes with transcription factors of the TCF/Lef family. A well-established functional read-out of Wnt signaling makes use of TCF responsive luciferase reporter constructs (Korinek et al., 1997). To test the functional relevance of the interaction between ß-catenin and RanBP3, we transfected human embryonic kidney cells (HEK293) with reporter constructs that contain either three optimal TCF binding sites (TOP) or three mutated binding sites (FOP). Transfection of a Wnt1 plasmid resulted in a strong activation of the TOP reporter but not of the FOP control (Fig. 2B). Co-transfection of increasing amounts of RanBP3 repressed Wnt1/ß-catenin transactivation dose-dependently (Fig 2B). A mutant of RanBP3 that cannot interact with RanGTP and

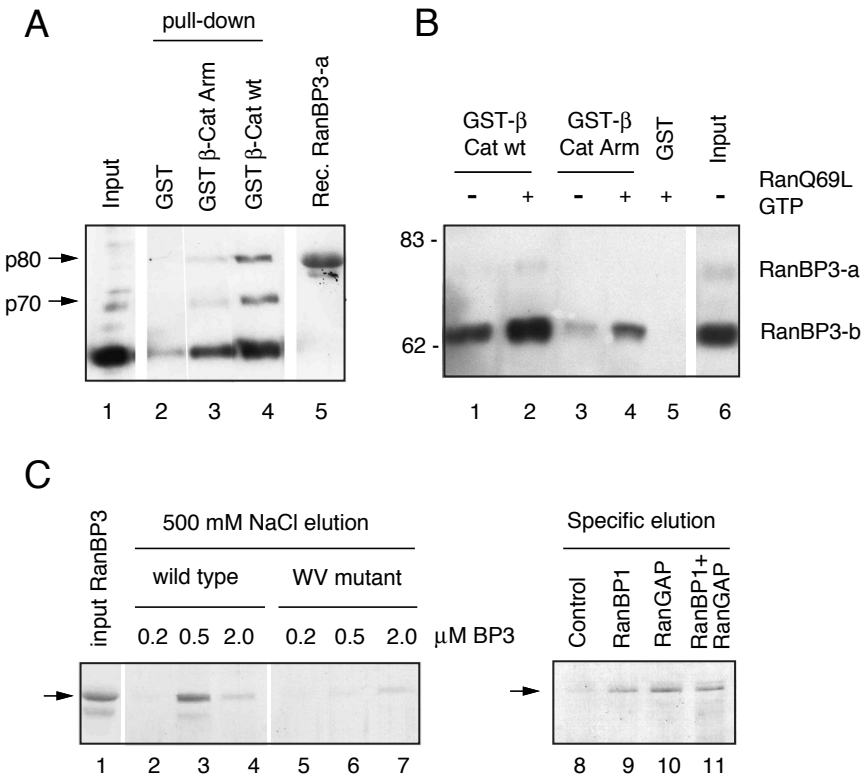

Figure 1. Identification of RanBP3 as an interaction partner of ß-Catenin. A. Pull down experiment using immobilized GST (lane 2), GST-tagged ß-Catenin ARM repeats 1-12 (lane 3) and full length ß-Catenin (lane 4) incubated with Xenopus egg extract (input, lane 1). Bound proteins were analyzed by Western blot using Mab 414 recognizing a subset of nucleoporins. Two unknown proteins p80 and p90 are marked with an arrow. B. Identification of p80 and p90 as the b and a isoforms of RanBP3. Pull down experiment as in A, incubated with HeLa nuclear extracts and analyzed using RanBP3 antibody. C. RanBP3 binds directly to ß-Catenin. GST-tagged full length ß-Catenin (lanes 2-11) was incubated with 2 µM RanGTP and 0.2 µM (lanes 2 and 5), 0.5 µM (lanes 3, 6, 8-11) or 2.0 µM (lanes 4 and 7) wild type (lanes 2-4, 8-11), or "wv" mutant (lanes 5-7) RanBP3-b. Bound proteins were eluted as indicated above the lanes and visualized with silver (lanes 1-7) or Coomassie (lanes 8-11) staining.

binds ß-catenin with less affinity (Fig. 1C) was less active than wild type RanBP3 (Fig. 2B). To investigate whether RanBP3 inhibits Wnt signaling downstream or upstream of ß-catenin, we mimicked Wnt signaling in HEK293 cells by expressing ß-catenin. RanBP3 could still specifically inhibit activation of the TOP reporter (Fig. 2C), while the RanBP3 "wv" mutant was less effective. These experiments show that RanBP3 inhibits TCF-dependent transcription by acting either on ß-catenin itself, or on regulators downstream of ß-catenin. We confirmed that the expression levels of our wild type and "wv" mutant RanBP3 constructs were equal by analyzing cell lysates from transfected HEK293 cells on Western blot (Fig. 2A).

The interaction of recombinant ß-catenin with RanBP3 (Fig. 1C) implies that RanBP3 can bind N-terminally unphosphorylated ß-catenin, which is thought to be the signaling-competent form of the protein. To test whether this is the case *in vivo*, we used a ß-catenin mutant that contains alanines in all four N-terminal GSK3ß phosphorylation sites (ß-cateninΔGSK3ß, Barth et al., 1999), and therefore is constitutively active. This mutant stimulated expression of the TCF reporter to 2-3 fold higher levels than wild type ß-catenin (data not shown). Co-expression of wild-type RanBP3 lead to a significant reduction in transactivation by ß-cateninΔGSK3ß (Fig. 2D). Again, the RanBP3 RanGTP-binding mutant was less able to repress ß-cateninΔGSK3ß mediated

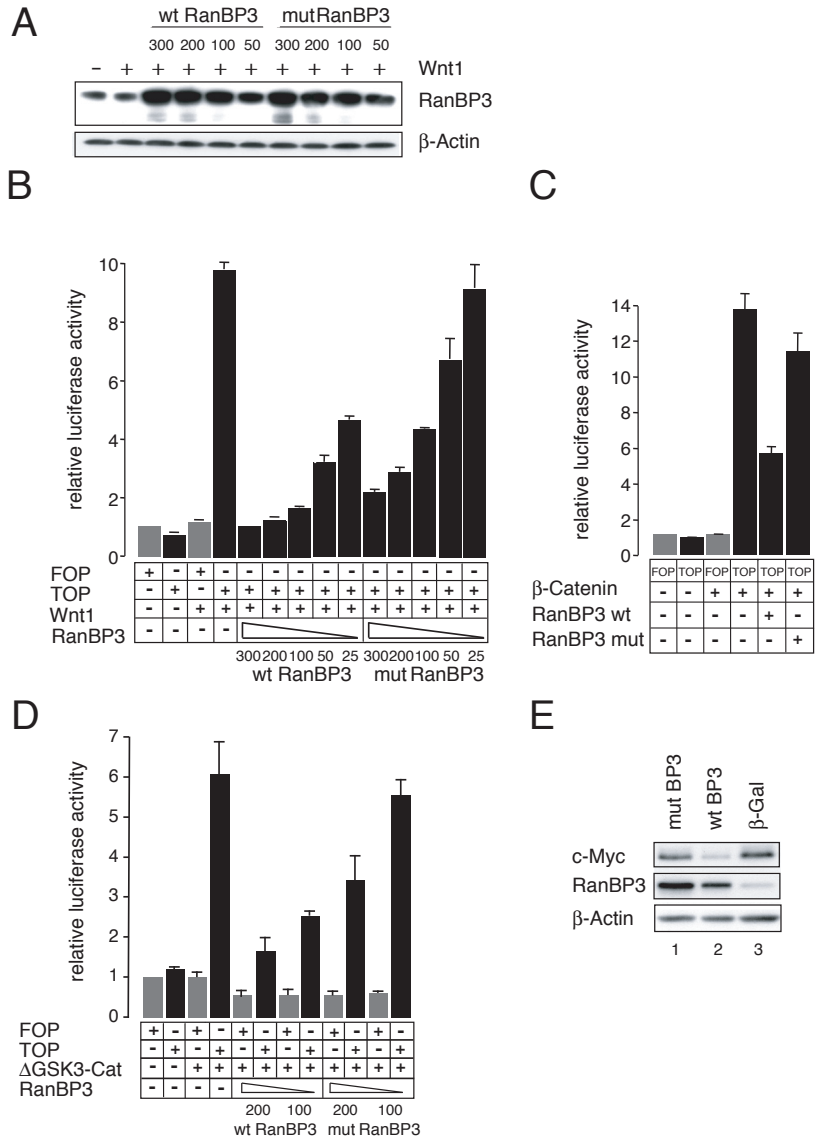

Figure 2. Expression of RanBP3 inhibits ß-Catenin/TCF mediated transcriptional activation. A. Wild type and "wv" mutant RanBP3 are expressed at equal levels. HEK293 cells were transfected with indicated constructs (ng) and lysates were analyzed 48 hrs post-transfection by Western blot with indicated antibodies. B. RanBP3 represses Wnt-1 induced ß-Catenin/TCF mediated transcriptional activation dose-dependently. HEK293 cells were transfected with TOP (black bars) or the control FOP (grey bars), Wnt1, and decreasing amounts of RanBP3 wt or "wv" mutant as indicated (ng) and luciferase activity was measured after 48 hours. C and D. RanBP3 represses transcriptional activation induced by wild type ß-Catenin (C) or ΔGSK3-ß-Catenin (D). HEK293 cells were transfected with indicated constructs and luciferase activity was measured 48 hrs after transfection. In all experiments, normalized relative luciferase values are shown as corrected with pRL-CMV Renilla. Bars represent standard errors of means of independent experiments E. RanBP3 inhibits the expression of the endogenous Wnt target c-Myc. HCT116 colon carcinoma cells expressing Δ45-ß-Catenin were transfected with GFP and ß-galactosidase, RanBP3 wt or mutant plasmids. 2 days after transfection, GFP-positive cells were sorted using flow cytometry, lysed in sample buffer and analyzed by Western blot using indicated antibodies.

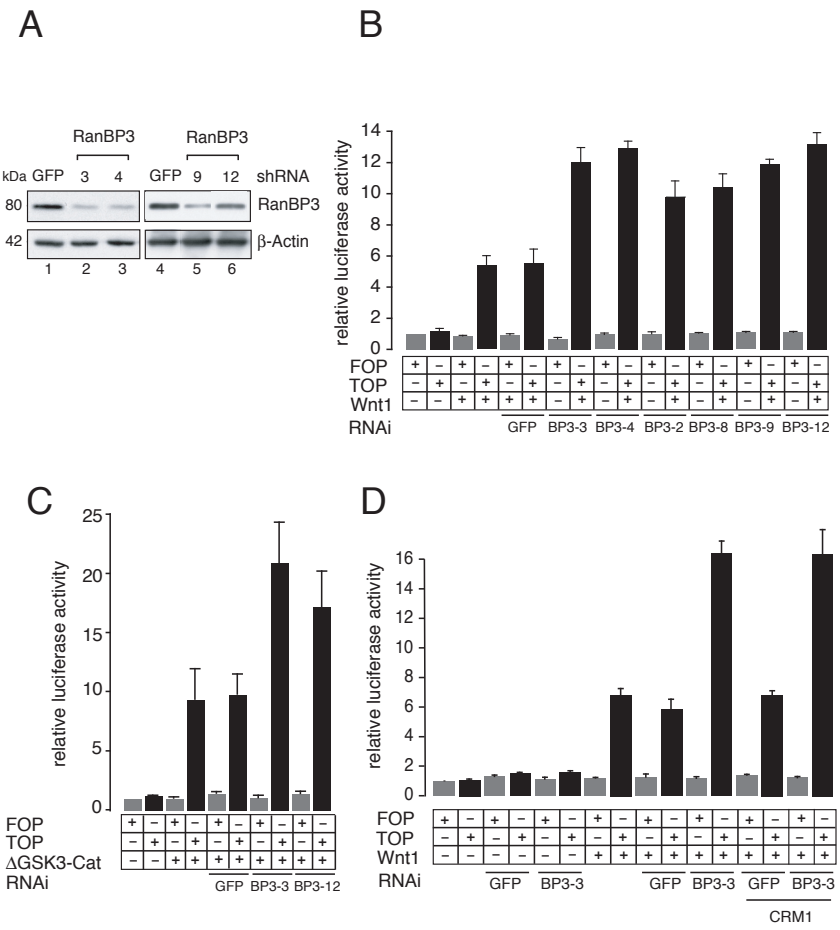

Figure 3. Reduction of RanBP3 by RNAi results in increased ß-Catenin/TCF mediated transcription activation. A. Western blot showing that different short hairpin RNAs (shRNA) against RanBP3 reduce RanBP3 protein levels in HEK293 cells. cells were transfected with shRNAs and pHA262-PUR was co-transfected to introduce puromycin resistence. 24 hrs after transfection, cells were grown on puromycin medium for 48 hrs and cell lysates were prepared and analyzed on Western blot with indicated antibodies B. RNAi against RanBP3 increases Wnt1-induced ß-Catenin/TCF-mediated transcription. HEK293 cells were transfected with indicated constructs and activity of TOP (black bars) and FOP (grey bars) were measured 72 hours after transfection C. RNAi against RanBP3 increases ß-Catenin/TCF driven transcription in HEK293 cells that transiently express an active form of ß-Catenin (ΔGSK3-ß-Catenin). Cells were transfected with indicated constructs and luciferase activity was measured after 72 hours. D. Co-expression of CRM1 with RanBP3 shRNA constructs does not affect ß-Catenin/TCF mediated transcription in Wnt1 transfected cells. HEK293 cells were transfected with indicated constructs and 72 hours after transfection luciferase activity was measured. For all experiments, relative luciferase levels are shown as corrected with CMV-Renilla-luc. Error bars in B represent standard deviations of technical replicates of a representative experiment. Bars in C and D represent standard errors of means of independent experiments.

transactivation.

To address whether RanBP3 could also affect expression of endogenous target genes of ß-catenin/TCF, we expressed RanBP3 in human colon carcinoma cell line HCT116. This cell line harbors an activating mutation in ß-catenin (Δ45 catenin) and therefore expresses increased levels of the target gene c-Myc (He et al., 1998). Expression of wt RanBP3 decreased c-Myc proteins levels compared to control cells (Fig 2E, lanes 2 and 3). Although expressed in higher levels, the wv mutant RanBP3 was less capable of

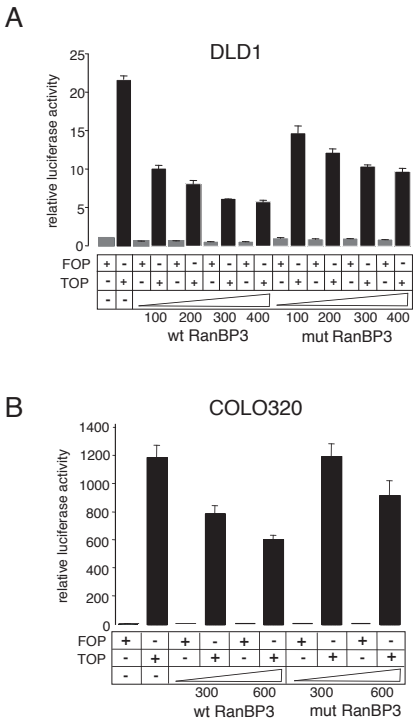

Figure 4. RanBP3 antagonizes Wnt/ß-Catenin transactivation in APC mutated colon carcinoma cells. Luciferase assay showing that RanBP3 inhibits ß-Catenin-mediated transactivation in colon carcinoma cell lines DLD1 and COLO320. A. APC type I truncated human colon carcinoma cell line DLD1 (APC 1-1417) was transfected with luciferase reporter constructs and increasing amounts of RanBP3 expression constructs as indicated. DLD1 cells express a truncated APC protein that lacks all its C-terminal NESs. B. Luciferase reporter assay as in A, carried out in the APC type I truncated human colon carcinoma cell line COLO320 (APC 1-811). These cells express a short APC protein that lacks all ß-Catenin binding and regulatory sites. Relative luciferase activity was measured 48 h post transfection. Bars represent standard deviations of a representative experiment.

decreasing c-Myc levels.

Reduction of RanBP3 results in increased transactivation of a TCF responsive reporter.
In addition to studying the effects of RanBP3 overexpression, we studied the effects of RanBP3 depletion. We expressed short hairpin RNAs (shRNAs) directed against different unique parts of RanBP3 that are present in all isoforms of RanBP3. We obtained several shRNA RanBP3 constructs that downregulate RanBP3 protein levels in HEK293 cells (Fig. 3A).
When we co-expressed Wnt1 and RanBP3 shRNAs, we observed significant increases in TCF/LEF reporter activity compared to the GFP RNAi control (Fig. 3B). To test whether RanBP3 depletion also acts on N-terminally dephosphorylated ß-catenin, we cotransfected ß-cateninΔGSK3ß with anti-RanBP3 shRNA expression constructs (Fig. 3C). Reduction of RanBP3 increased reporter activity, confirming that RanBP3 can act on the N-terminally dephosphorylated or "activated" form of ß-catenin. In the absence of Wnt signaling, depletion of RanBP3 did not result in increased reporter activity (Fig. 3D), arguing for a specific effect on ß-catenin. The direct binding of RanBP3 to ß-catenin that we observed (Fig. 1C) indicated that RanBP3 may act on the Wnt signaling pathway independently of CRM1, that has been reported to play a role in ß-catenin nuclear export via interaction with APC (Henderson, 2000; Neufeld et al., 2000; Rosin-Arbesfeld et al., 2000). Increased expression of CRM1 is able to compensate for reduction of CRM1 nuclear export at reduced RanBP3 levels (Taura et al., 1998); (Noguchi et al., 1999)). Therefore, we expressed CRM1 in combination with Wnt1 and RanBP3 shRNAs. As shown in Fig. 3D, CRM1 overexpression did not reverse the effects of RanBP3 depletion, indicating that the mechanism by which Wnt signaling is modulated by RanBP3 is independent of CRM1-mediated nuclear export of ß-catenin.

RanBP3 downregulates ß-catenin-mediated transactivation independently of APC.
To further address the question whether RanBP3 represses ß-catenin transcriptional activation by stimulating export of ß-catenin via the APC/CRM1 pathway, we expressed RanBP3 in human colorectal cancer cell lines that express C-terminal truncations of APC. First, we tested DLD1 cells, which express APC1-1417 that retains some ß-catenin binding sites but lacks all C-terminal nuclear export signals (NES) which are the ones most highly conserved in evolution. As shown in Fig. 4A, ß-catenin/TCF activity is already high in these cells. Expression of RanBP3 wt or "wv" mutant could still dose dependently downregulate transcriptional activity, the mutant again being a less potent inhibitor (Fig. 4A). As APC in DLD1 cells can still bind to ß-catenin, and NESs have also been reported in the N-terminus of APC, we repeated the experiment in COLO320 cells. These cells express a very short APC truncation (1-811) that lacks all ß-catenin binding sites. ß-catenin/TCF activity was much higher in

these cells than in DLD1 cells correlating with the severity of the APC mutation (Fig. 4B, Rosin-Arbesfeld et al., 2003). Nevertheless, transfection of the RanBP3 expression constructs caused a significant downregulation of transcription (Fig. 4B). Therefore, the mechanism by which RanBP3 inhibits ß-catenin is independent of a nuclear export function of APC.

RanBP3 influences subcellular localization of active ß-catenin

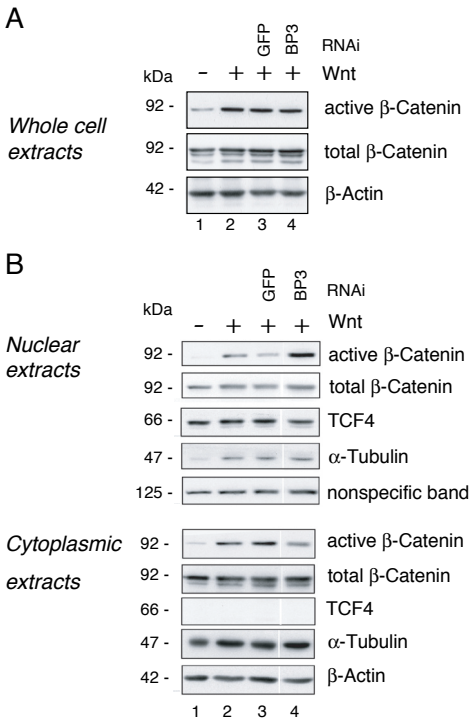

Figure 5. Depletion of RanBP3 results in nuclear accumulation of active ß-Catenin. A. Depletion of RanBP3 does not alter the levels of both total and active dephosphorylated ß-Catenin. HEK293 cells were transfected with or without Wnt1 and shRNA constructs against GFP or RanBP3. 72 hours after transfection, whole cell lysates were analyzed by Western blot with indicated antibodies. B. RNAi against RanBP3 results in increased levels of active ß-Catenin in the nucleus. HEK293 cells were transfected with indicated constructs and 72 hours post transfection nuclear and cytoplasmic extracts were prepared and analyzed by Western blot. TCF4 and Tubulin staining are shown as markers for purity of the nuclear and cytoplasmic fractions. As a loading control in the nuclear fractions TCF4 and a non-specific reaction of the antibody recognizing active ß-Catenin are shown.

To study the mechanism by which RanBP3 inhibits Wnt signaling, we tested the possibility that RanBP3 influences the stability of ß-catenin. We transfected HEK293 cells with or without Wnt1 in combination with shRNA constructs. Total ß-catenin levels were virtually unchanged after expression of Wnt1 alone or in combination with shRNA against RanBP3 (Fig. 5A). When the same blot was probed with anti-active ß-catenin, recognizing N-terminally desphosphorylated ß-catenin, we observed an increase in Wnt1 transfected cells but no effects of RanBP3 (Fig. 5A). From this we conclude that RanBP3 depletion does not affect ß-catenin degradation.

We next prepared nuclear and cytoplasmic extracts from HEK293 cells transfected with or without Wnt1 and RNAi against GFP or RanBP3. Total ß-catenin was mostly detected in the cytosol fraction (Fig. 5B). No change in total ß-catenin levels was observed in the nucleus or cytoplasm after transfection with Wnt1 (Fig 5B, lane 2), or treatment with RNAi (lanes 3 and 4). When we stained for active ß-catenin, a clear increase was evident after stimulation with Wnt1 (Fig. 5B, lane 2). Interestingly, when cells were transfected with RNAi against RanBP3, active ß-catenin significantly increased in the nuclear fraction and decreased in the cytosolic fraction (Fig. 5B, lane 4), suggesting that RanBP3 relocates active ß-catenin from the nucleus to the cytoplasm. As controls for fractionation, TCF4 was used as a nuclear marker and α-Tubulin as a cytoplasmic marker. Both proteins were strongly enriched in the proper compartments.

Nuclear/cytoplasmic fractionation data does not allways reflect the subcellular localization in living cells, as pools of proteins that are not tightly bound to nuclear or cytoplasmic structures and are relatively small may leak through NPCs of permeabilized cells. We therefore assayed the effect of RanBP3 overexpression on active ß-catenin in situ using the anti-active ß-catenin antibody. In our hands, this antibody did not visualize endogenous dephosphorylated ß-catenin in Wnt1 transfected HEK293 cells (data not shown). We therefore tested two colon carcinoma cell lines, SW480 and DLD1 that have a constitutively activated ß-catenin due to a mutation in APC (Rosin-Arbesfeld et al., 2003). In SW480, but not in DLD1, the anti-dephospho-ß-catenin antibody recognizes a clear nuclear signal above background (Fig. 6A and C). The presence of this signal correlates with the exceptionally high ß-catenin activity as measured in luciferase assays (Fig. 6D), that is approximately 30 fold higher than in DLD1. Importantly, RanBP3 overexpres-

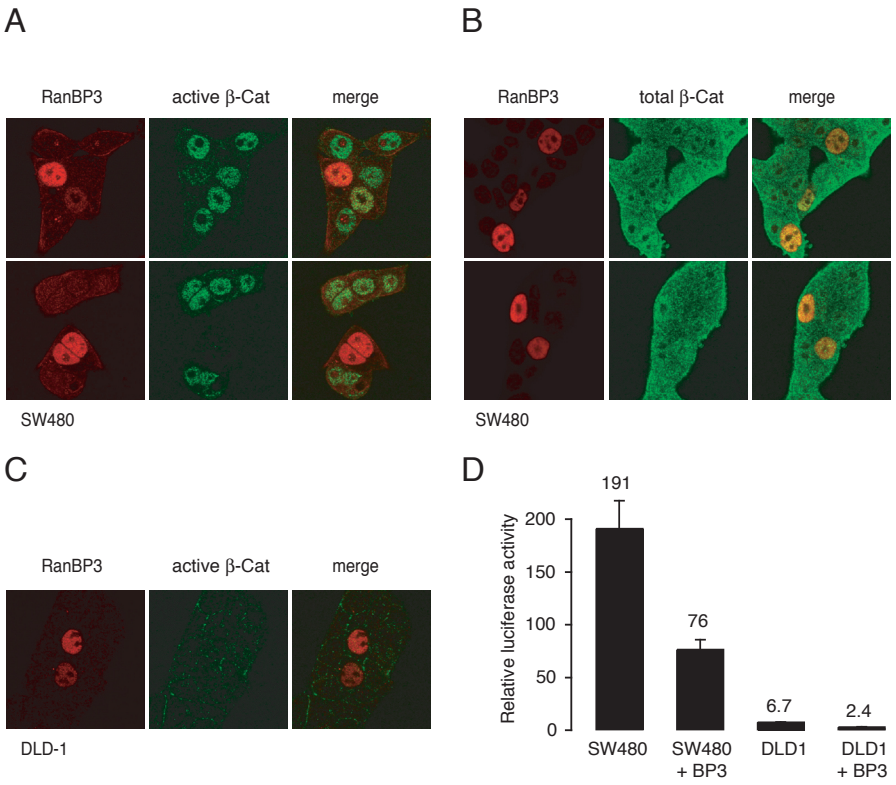

Figure 6. RanBP3 induces specific depletion of endogenous nuclear active ß-Catenin. SW480 (A, B) or DLD1 (C) colon carcinoma cells were transfected with RanBP3 expression plasmids and stained after 45h for dephospho-ß-Catenin (A and C) or total ß-Catenin (B). RanBP3 expression was visualized in the same cells using a RanBP3 polyclonal (A and C) or monoclonal antibody. D. Luciferase reporter assay as in Fig. 2-4 measuring relative ß-Catenin activity. Cells were transfected as in A and C; Error bars represent standard deviations of technical replicates.

sion leads to a clear reduction of active ß-catenin signal from the SW480 nuclei (Fig. 6A), but has no influence on total ß-catenin localization (Fig. 6B). This indicates that, even in the extremely active SW480 cell line, only a very small proportion of total ß-catenin is properly dephosphorylated and active, and that this is the pool RanBP3 acts upon.

RanBP3 enhances nuclear export of active ß-catenin independently of CRM1

Reduction of active nuclear ß-catenin by RanBP3 in SW480 cells was not accompanied by an increase in cytoplasmic signal, raising the question whether RanBP3 induces enhanced nuclear export of active ß-catenin or its increased phosphorylation. However, enhanced nuclear export would result in dilution in a cytoplasmic volume that is roughly ten fold larger than that of the nucleus, precluding detection by the anti-dephospho-ß-catenin antibody. To discriminate between the two possibilities, we mimicked the active state of ß-catenin using a monomeric RFP (mRFP) tagged, constitutively active form of ß-catenin, the previously employed ß-cateninΔGSK3ß. To test whether this fusion protein was biologically active, we performed a TCF-reporter assay in the malignant mesothelioma cell line NCI-H28, which carries a homozygous deletion of the ß-catenin gene (Calvo et al., 2000). This prevented possible activating effects of this mutant on endogenous ß-catenin. mRFP-ß-cateninΔGSK3ß activated the very low endogenous TCF activity of these cells to a great extent (Figure 7B). We next compared the subcellular localization of this protein in the presence or absence of exogenous RanBP3 (Fig. 7A). Care was taken to record cells of similar low expression levels (Fig. 7C). In control cells, more mRFP-ß-cateninΔGSK3ß was present in the nuclei compared to the cytoplasm (median nuclear

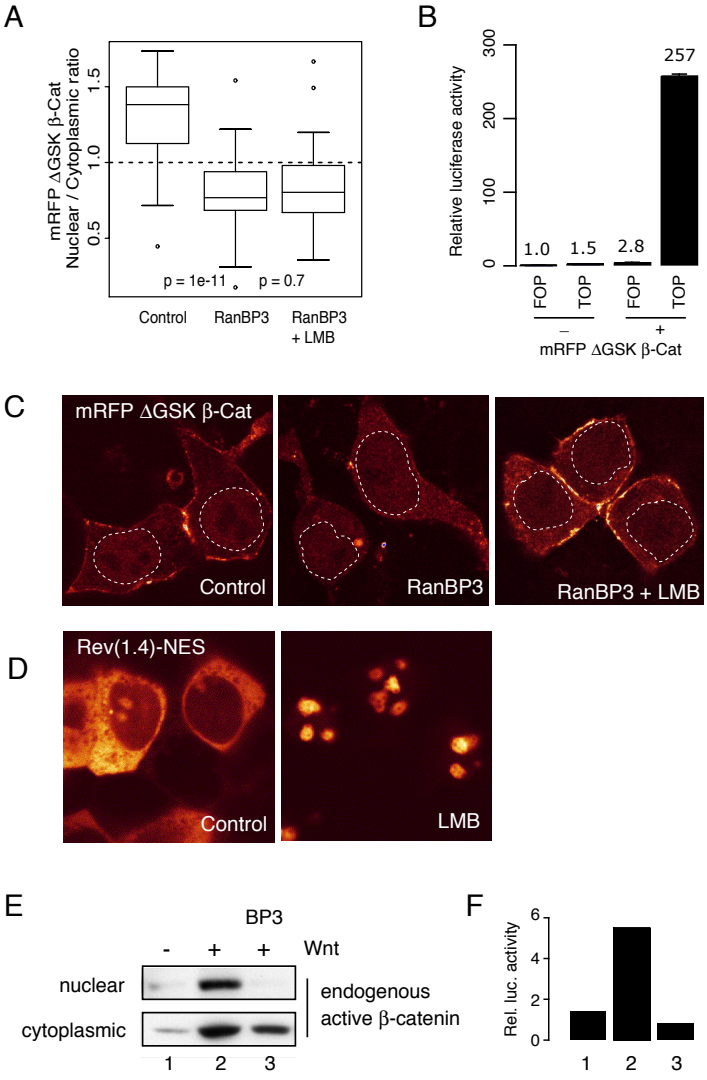

Figure 7. RanBP3 enhances nuclear export of active ß-Catenin independently of CRM1. A and C. Effect of RanBP3 on mRFP-ΔGSK ß-Catenin nucleocytoplasmic distribution in HEK293 cells in presence or absence of 50 nM LMB for 3h. A. Box plot showing the distribution of nuclear-cytoplasmic ratios of mRFP-ΔGSK ß-Catenin of two independent experiments. P values are according to Mann-Whitney tests. Representive mRFP fluorescence images are shown in C. Highlighted nuclear borders are drawn on the basis of accompanying phase contast images. B. Functionality of mRFP-ΔGSK3-ß-Catenin. NCI-H28 cells (lacking endogenous ß-Catenin) were transfected with indicated constructs and 48 hours after transfection luciferase activity was measured. Shown are relative luciferase levels as corrected for transfection efficiency (Renilla luciferase activity). Bars represent standard deviations. D. Representive fluorescence images of HEK293 cells expressing GFP-Rev(1.4)-NES in the presence or absence of 50 nM LMB for 3h. E and F. Endogenous activated ß-Catenin relocalizes from the nucleus to the cytoplasm upon over-expression of RanBP3. HEK293 cells were transfected with Wnt and RanBP3 as indicated together with TOP-TK-luc and Renilla transcription reporter plasmids and fractionated after 48h as in Fig. 5. Localization of active ß-Catenin was monitored using anti-active ß-Catenin antibody. Amounts of protein loaded were normalized on transfection efficiency (Renilla luciferase activity). Normalized ß-Catenin/TCF dependent luciferase activity is depicted in F.

to cytoplasmic ratio of 1.38, n=37).
In contrast, cells expressing exogenous RanBP3 showed a higher cytoplasmic than nuclear mRFP-ß-cateninΔGSK3ß levels (median nuclear to cytoplasmic ratio of 0.77, n = 41). Importantly, addition of 50 mM of the CRM1 inhibitor leptomycin B (Wolff et al., 1997) did not significantly change the effect of RanBP3 (median nuclear to cytoplasmic ratio of 0.80, n=52), eventhough photobleaching experiments show that mRFP-ß-cateninΔGSK3ß rapidly shuttles between the nucleus and cytoplasm (data not shown). Identical LMB treatment dramatically relocalized the NES-containing reporter protein Rev(1.4)-NES-GFP (Henderson and Eleftheriou, 2000) to the nucleus (Fig. 6D). We conclude that RanBP3 enhances nuclear export of active ß-catenin, and that this export is independent of CRM1. To confirm that endogenous activated ß-catenin relocalises from the nucleus to the cytoplasm upon overexpression of RanBP3 in HEK293 cells, we transfected these cells with Wnt1 and RanBP3. Indeed, we observed increased active ß-catenin levels in both nuclear and cytoplasmic fractions, of which the nuclear pool was more sensitive to RanBP3 overexpression than the cytoplasmic pool (Fig 7E). The decrease in cytoplasmic active ß-catenin is consistent with increased nuclear export of ß-catenin and subsequent degradation in the cytoplasm.

RanBP3 suppresses dorsal-ventral axis formation in *X. embryos*

To study the role of RanBP3 in Wnt signaling in a physiological context, we used a *X. laevis* axis duplication assay. During *X. laevis* embryonic development, Wnt signaling determines patterning along the dorsal ventral axis. Ectopic ventral injection of ß-catenin mRNA in 4-cell embryos resulted in clear axis duplication (Fig. 8A,B). The majority of the embryos (75%) showed a complete duplication of the dorsoventral axis. 22% of the embryos showed a partial duplication i.e. secondary axis without duplicated cement gland. However, co-injection of ß-catenin mRNA with RanBP3 mRNA resulted in a strong suppression of the double axis phenotype in the majority of the embryos (63%). Only few partial or very partial secondary axis (24% and 13% respectively) were observed in these embryos (Fig. 6B). We also co-injected ß-catenin mRNA with mRNA of the RanBP3 “wv” mutant that is defective in RanGTP binding. This mutant suppressed the double axis phenotype but was not such a potent inhibitor as the wild type RanBP3 (Fig. 8A, B; p=4e-8). This data correlates with our findings that this RanBP3 mutant binds ß-catenin with less affinity (Fig. 1) and that it is less active in repressing transcriptional activity of a TCF reporter gene in human cell lines (Fig. 2 and 4). If RanBP3 is an inhibitor of nuclear ß-catenin function, dorsal injection of RanBP3 mRNA is expected to result in ventralization of the embryo. We therefore injected 4-cell embryos dorsally with either RanBP3 or control mRNA and scored ventralization after three days of development by dorso-anterio index (DAI). Mild to severe ventrilization was observed (DIA1-4) in 80% of RanBP3 injected embryos (Fig 8C), while only less then 10% of control injected embryos showed these phenotypes. Complete ventrilization (DIA0) was not observed. An important direct downstream target of dorsal nuclear ß-catenin acitvity is the early Wnt-inducible homeobox gene Siamois (Brannon et al., 1997). We therefore tested whether expression levels of this gene were reduced in the RanBP3 injected embryos by RT-PCR. In four independent experiments, we detected a ~2 fold decrease in Siamois levels in late stage 9 embryos (Figure 8D and E). This decrease is rather mild, consistent with the incomplete ventralization phenotypes observed. Together, we conclude that RanBP3 is not only a repressor of Wnt signaling in human cell lines but it also functions as an antagonist of Wnt signaling in *X. laevis* embryos.

Loss of function of *ranbp3* results in a naked cuticle phenotype in *D. melanogaster*

Wnt signaling is highly conserved between different species. We identified the Drosophila RanBP3 homologue and used RNAi to study its role in Drosophila development. At the end of embryogenesis, the ventral epidermis is covered by a cuticle that is built up by a repeating pattern of naked cuticle and denticles (Fig. 9A). Wingless (Wg, Drosophila Wnt) signaling increases levels of Armadillo (ß-catenin) that specifies the fate of epidermal cells responsible for secreting naked cuticle. Therefore, loss of wg expression results in an embryo that is covered with denticles lacking naked cuticle (Nusslein-Volhard and Wieschaus, 1980) and overexpression of wg results in a naked cuticle embryo (Noordermeer et al., 1992). Likewise, loss of an inhibitor of Wnt signaling also results in naked cuticle embryos as shown by e.g. RNAi against Daxin (Willert et al., 1999). As a control, we injected embryos with ß-galactosidase double stranded RNA (dsRNA) and observed that the majority (97%) developed into larvae that were indistinguishable from non-injected wild-type larvae (Fig. 9A). 3% of these control embryos showed some very weak effects

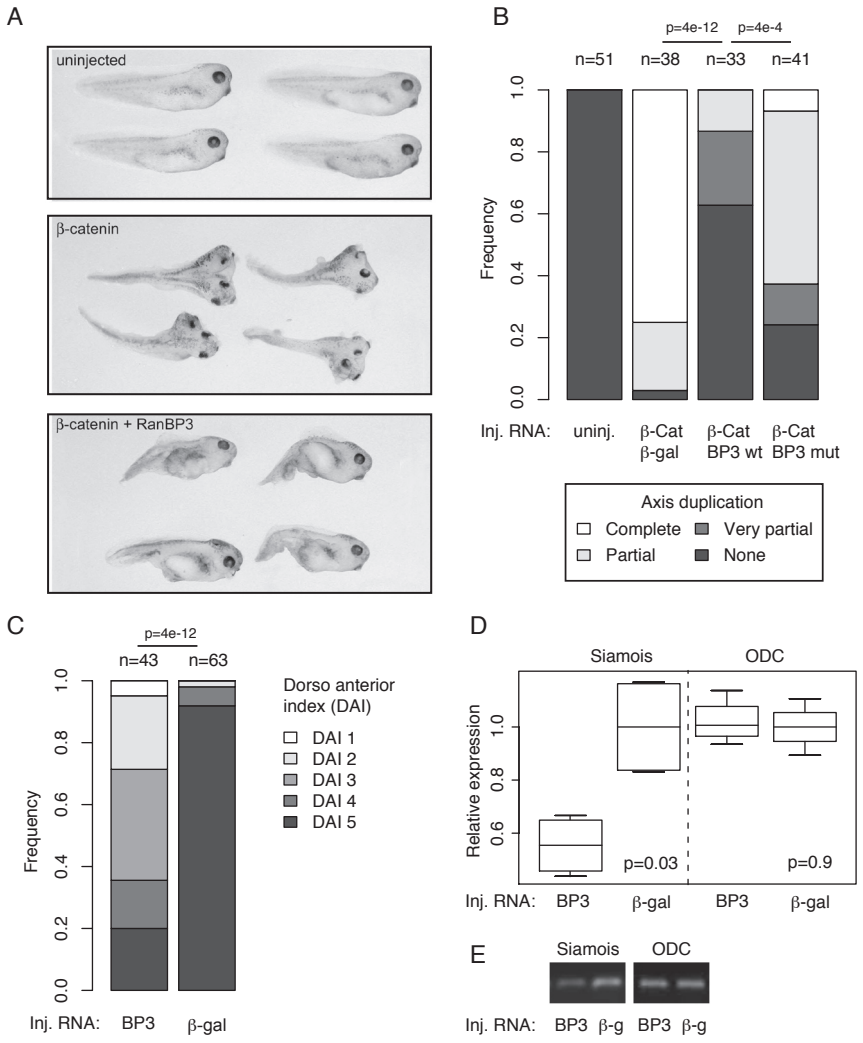

Figure 8. RanBP3 rescues ß-Catenin-induced double axis formation in *X. laevis* embryos. A. *X. laevis* embryos were injected ventrally at the 4-cell stage with ß-Catenin mRNA, in the presence or absence of control ß-galactosidase or Xenopus RanBP3-b mRNA. In the upper panel wild type non-injected embryos are shown. Middle panel shows double axis phenotype as induced by the injection of ß-Catenin mRNA. Lower panel shows embryos that are rescued from the double axis phenotype by co-expression of RanBP3 and ß-Catenin mRNA. B. Quantification of the different phenotypes of two independent experiments in four categories: complete secondary axis (with cement gland), partial secondary axis (i.e. any secondary axis lacking the cement gland), vestigial axis (very small posterior protrusion or pigmented line) and normal (only one axis). P values are according to Pearson's Chi-squared test for count data. C. Dorsal injection of RanBP3 results in ventralization of Xenopus embryos. 4-cell stage embryos were injected dorsally with RanBP3 or control (ß-galactosidase) mRNA and analyzed three days later for ventralization using the standarized dorso-anterior index (DAI)(Kao and Elinson, 1988). This scale runs from 0 (complete ventralization) to 5 (normal development). Frequencies are derived from three independent experiments. P-values as in B. D. The ß-Catenin downstream target siamois is significantly downregulated in RanBP3 injected embryos. Embryos were injected as in C and analyzed for siamois or ornithine decarboxylase (ODC) mRNA using RT-PCR. Amplified ethidium bromide stained DNA of four experiments was quantified and normalized to mean signals from ß-galactosidase injected embryos and represented in a boxplot. P-values are according to Mann-Whitney tests. E. Representive signals from RT-PCR reactions visualized by ethidium bromide staining.

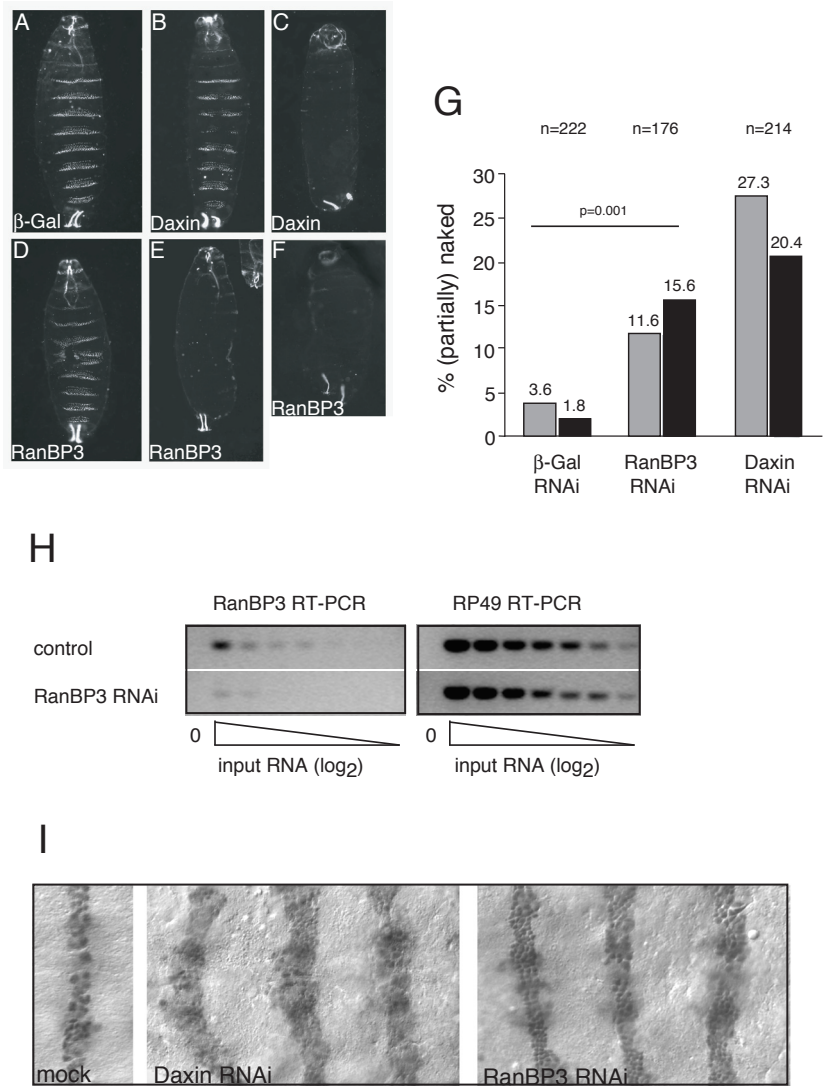

Figure 9. Loss of RanBP3 by RNAi results in a naked cuticle phenotype in Drosophila. Shown are dark field images of cuticle preparations of control (β-galatosidase) (A), Drosophila Daxin (B and C) and Drosophila RanBP3 dsRNA injected embryos (D, E, F). Loss of Daxin and RanBP3 results in increased Wnt signaling and replacement of denticles by naked cuticle. Partially naked cuticles (B and D), nearly naked (E) cuticles and naked cuticles (C and F) are shown. All views are ventral, top is posterior. G. Quantification of two representative experiments showing the frequency of the cuticle phenotype. P-values are calculated as in Figure 7B. Note that the contribution of the completely naked phenotype in the RanBP3 RNAi embryos is relatively high (results not shown). H. RT-PCR showing reduction in RanBP3 mRNA levels in RanBP3 dsRNA injected embryos. Embryos were injected as in A. and RNA was extracted after 15h of development. RT-PCRs specific for RanBP3 or control (ribosomal protein RP49) were performed using nothing (0) or a series of 2 fold dilutions of extracted RNA. I. Loss of RanBP3 function by dsRNA injection results in increased expression of the wg target gene engrailed. Shown are Engrailed antibody staining of buffer injected embryo (left), Daxin dsRNA injected embryo (middle) and RanBP3 dsRNA injected embryo (right). Note that the buffer injected embryo developed until late stage 11 whereas the Daxin and RanBP3 RNAi embryos shown are stage 10 embryos, explaining the larger cells in the former embryo. The number of Engrailed positive cell rows between stage 10 and 11 is identical. Ventral-lateral view is shown, posterior is left.

on denticle belt formation (Fig. 9G).
RNAi against the (Daxin) resulted in a significant increase in naked cuticle phenotype in 24% of the Daxin dsRNA injected embryos (Fig. 9G) with phenotypes varying from partial loss of denticles to completely naked embryos (Fig. 9B and C). Injection of dsRNA against the *D. melanogaster* RanBP3 caused a partial or complete transformation of denticles into naked cuticle in 14% of the embryos (Fig. 9D-F). The most severe phenotypes of the RanBP3 RNAi embryos showed deformation of both the head and spiracles (Fig. 9F), resembling Daxin RNAi (Fig 9C). In addition, almost all RanBP3 RNAi embryos showing a strong naked cuticle phenotype were shorter than the embryos injected with Daxin dsRNA. To confirm that the RanBP3 dsRNA injections resulted in decreased RanBP3 levels, we performed RT-PCRs on buffer and RanBP3 dsRNA injected embryos. Fig. 9H shows that RanBP3 mRNA levels were indeed decreased in RanBP3 dsRNA injected embryos while RP49 control mRNA levels remained unaffected. We then assayed the effects of RanBP3 dsRNA injection on wg target gene induction. For this, stage 10 RanBP3 or Daxin dsRNA injected embryos were stained with anti-Engrailed antibody. Normal engrailed expression is present in segmental stripes that are two cells wide (Fig. 9I, left). Removal of the Wnt signaling inhibitor Daxin by dsRNA injection resulted in a broader Engrailed expression pattern that extended from 2 to 4 rows of cells (Fig. 9I; middle). In RanBP3 dsRNA injected embryos, Engrailed expression expanded by one row of cells (Fig. 9I, right). These *in vivo* data show that removal of RanBP3 leads to a phenotype that is associated with Wnt signaling activation, suggesting that RanBP3 also acts as negative regulator of Wnt signaling in *D. melanogaster.*

Discussion

In this study, we identify RanBP3 as a novel inhibitor of Wnt signaling that acts on ß-catenin directly by enhancing nuclear export of its active form. We show that RanBP3 binds directly to ß-catenin and that the interaction is increased in the presence of RanGTP. Expression of RanBP3 represses Wnt signaling both *in vitro* and in *X. laevis* embryonic development. Inhibition of RanBP3 by RNAi causes over-activation of Wnt signaling in tissue culture cells and in *D. melanogaster* embryos. In addition, expression of RanBP3 in human cells specifically reduces active ß-catenin levels in the nucleus and relocates ΔGSK3-ß-catenin from the nucleus to the cytoplasm, independently of CRM1.
RanBP3 was originally identified as a nuclear protein that contains FG repeats and a RanGTP-binding domain (Mueller et al., 1998). RanBP3 can directly bind the nuclear export receptor CRM1, stimulating the formation of nuclear export complexes and increasing the export rate of certain CRM1 substrates (Englmeier et al., 2001; Lindsay et al., 2001). One mechanism by which RanBP3 could influence ß-catenin activity would therefore be increased nuclear export via the CRM1 pathway. Although the nuclear export mechanisms of ß-catenin are not fully understood, two pathways have been proposed (Henderson and Fagotto, 2002). In the first, ß-catenin exits the nucleus independently of nuclear export receptors by interacting directly with proteins of the nuclear pore complex (Wiechens and Fagotto, 2001; Eleftheriou et al., 2001). In the second pathway, ß-catenin exits the nucleus via the CRM1 pathway, but as ß-catenin does not contain NESs of its own, it uses binding to APC to exit the nucleus. The APC tumor suppressor does contain functional NESs and has been shown to be exported by CRM1 (Henderson, 2000; Neufeld et al., 2000; Rosin-Arbesfeld et al., 2000). Therefore, RanBP3 could inhibit ß-catenin by stimulating its export via APC and CRM1. However, four lines of evidence argue against this. First, in a CRM1 export complex, RanBP3 would bind to the complex via CRM1. Instead, we find that RanBP3 interacts directly with ß-catenin. Second, ß-catenin activity is RanBP3-sensitive in colon carcinoma cell line COLO320 (Quinn et al., 1979) that expresses a short type I APC truncation lacking all ß-catenin interaction sites (Rosin-Arbesfeld et al., 2003). We cannot formally exclude that the neuronal APC-like protein APC2 (van Es et al., 1999), which is expressed in certain colon carcinoma cell lines compensates for loss of APC. However, in luciferase reporter assays, CRM1 overexpression does not reverse stimulation of ß-catenin activity caused by depletion of RanBP3. Finally, RanBP3 mediated relocalization of active ß-catenin is insensitive to leptomycin B, a potent CRM1 inhibitor (Wolff et al., 1997). Therefore, we conclude that the mechanism by which RanBP3 inhibits ß-catenin is independent of CRM1 and APC.
Recently, it has been suggested that nuclear ß-catenin signaling is carried out mainly by ß-catenin dephosphorylated at serine 37 and threonine 41, which are main target sites of GSK3ß (Staal et al., 2002; van Noort et al., 2002). Depletion of RanBP3 by RNAi specifically increases the amount of dephosphorylated ß-catenin in

nuclear fractions, while RanBP3 overexpression has the opposite effect. No concomitant increase of cytoplasmic endogenous active ß-catenin was observed by overexpression of RanBP3, rather a small decrease. We attribute this to cytoplasmic phosphorylation and subsequent degradation of wild-type ß-catenin.

Endogenous active ß-catenin was visualized in situ, using the anti-active ß-catenin antibody recognizing desphosphorylated ß-catenin. This was only possible in SW480 colon carcinoma cells that contain a high level of active ß-catenin, due to severely defective APC function (Korinek et al., 1997). RanBP3 overexpression reduced active ß-catenin levels in the nucleus, but had no effect on total ß-catenin. This suggests that only a small proportion of total ß-catenin is active in SW480 cells and confirms the specificity of RanBP3 for active ß-catenin. Apparently, absence of proper ß-catenin phosphorylation and degradation is not sufficient for ß-catenin to be in an active, dephosphorylated state. Also, we infer that the modulation by RanBP3 of ß-catenin activity as measured in our luciferase reporter assays acts on a small dephosphorylated pool, explaining why RanBP3 modulates wild-type and ΔGSK3 ß-catenin to a similar extend (Fig. 2 and 4).

To discriminate whether RanBP3 enhances ß-catenin N-terminal phosphorylation or nuclear export, we have visualized both nuclear and cytoplasmic distribution of active ß-catenin. For this, we used a fluorescently tagged ß-cateninΔGSK3 that is resistant to N-terminal phosphorylation and degradation. As shown in Figure 7, RanBP3 causes a clear and highly significant shift of ß-cateninΔGSK3 from the nucleus to the cytoplasm. We therefore conclude that RanBP3 directly enhances nuclear export of active ß-catenin. How does RanBP3 perform this task? Recent studies have indicated that the interactions of nuclear factors with chromatin or with each other are highly dynamic (Dundr et al., 2002; Phair et al., 2004). This suggests that RanBP3 does not need to actively remove ß-catenin from the TCF/LEF-chromatin complexes. We therefore favor the possibility that association with RanBP3 prevents association of active ß-catenin with chromatin and keeps it in a more soluble state. In itself, this would be sufficient to allow CRM1-independent nuclear exit. We do not know whether RanBP3 accompanies ß-catenin to the cytoplasm and acts as a true nuclear export factor. The stimulatory effect of RanGTP on the ß-catenin/RanBP3 interaction, and the consistently weaker inhibitory effects on ß-catenin of a RanBP3 mutant unable to bind RanGTP would argue in favor of this possibility. Hydrolysis of RanGTP in the cytoplasm would increase the efficiency of release of ß-catenin for subsequent interactions with the cytoplasmic interacting proteins, such as E-cadherin or the APC/Axin/GSK3ß complex.

We studied the effect of RanBP3 in *X. laevis* and *D. melanogaster* embryogenesis. Overexpression of the *X. laevis* homologue of RanBP3 during early embryogenesis inhibits ß-catenin-dependent dorsoventral axis formation. RNA interference of the *D. melanogaster*homologue of RanBP3 causes naked cuticle phenotypes and a broader Engrailed expression domain due to overactivation of the Wnt signaling pathway. Therefore, the results obtained in these two model organisms support the results obtained in cultured human cell lines and indicate that the inhibitory function of RanBP3 is highly conserved in metazoan evolution.

Wnt signaling plays an important role in tumor initiation and progression in a variety of human solid tumors, including colon carcinomas, hepatocellular carcinomas and melanomas (Bienz and Clevers, 2000; Polakis, 2000). As a negative modulator of Wnt signaling, RanBP3 is a novel candidate tumor suppressor protein. Interestingly, the RanBP3 gene is located 19p13.3, a region that is commonly deleted in several types of cancer and in which multiple tumor suppressor genes are likely to be present (Lee et al., 1998); (Oesterreich et al., 2001); (Tucci et al., 2001); (Yanaihara et al., 2003); (Miyai et al., 2004); (Kato et al., 2004); (Yang et al., 2004). Further work is required to determine if loss of the RanBP3 gene contributes to these or other types of cancer.

In conclusion, we have identified an unexpected role for RanBP3 as a novel inhibitor of Wnt signaling that enhances nuclear export of active ß-catenin. This function is separate from its role in CRM1-mediated nuclear export. The structural similarities between CRM1 and ß-catenin suggest that RanBP3 may be a more general cofactor for nuclear export of Armadillo repeat proteins.

Materials and Methods

Data analysis

Statistical analysis was done using the R software package (R Development Core Team, 2005).

Reagents

Antibodies used were ß-catenin (C19220) (Trans-

duction Lab.) and H-102 (Santa Cruz), RanBP3 (R33620) (Transduction Lab.) and PA1-084 (Affinity Bioreagens), active ß-catenin (ABC 8E7), TCF4 (6H5-3) (Upstate), 414 (Eurogentec/Babco), α-Tubulin (YL1/2, ECACC), Actin (Ab-1, Oncogene) and c-Myc (9E10, Santa Cruz). The 4D9 anti-Engrailed/invected mAb was a gift from Corey Goodman (Patel et al., 1989).

Plasmids
The following plasmids were used: GST-ß-catenin and GST-ARM (Wiechens and Fagotto, 2001), pET14b-h-RanBP3-b (Mueller et al., 1998), pET14b-h-RanBP3-b "wv" mutant (Englmeier et al., 2001), pRev(1.4)-RevNES-GFP (Henderson and Eleftheriou, 2000). pQE32-Ran and pQE32-RanQ69L were kind gifts from D. Görlich (ZMBH Heidelberg, Germany). TOP/FOP-Tk and Wnt1, GFP-ß-catenin and pSUPER plasmid were kind gifts from H. Clevers (Hubrecht Laboratory, Utrecht, The Netherlands), R. Kypta (UCSF, San Fransisco, USA) and R. Agami (NKI, Amsterdam, The Netherlands). pcDNA3-RanBP3-b wt and pcDNA3-RanBP3-b "wv" mutant were constructed by generating a blunt NdeI/EcoRV fragment from pET14b-h-RanBP3-b wt and "wv" mutant and by inserting these fragments into the EcoRV site of pcDNA3 (Invitrogen). shRNAs were expressed from the pSUPER vector (Brummelkamp et al., 2002). The successful 19 nt target sequences were: RanBP3 2: AAGGCGGAGAAGATTCTGACA 3: AAAGAGCCCCAGAAAAATGAG, 4: AAGAGCCCCAGAAAAATGAGT, 8: AAGCCGACATGGAGAATG-CTG, 9: AACCGCAACGAACTATTTCCT, 12: AAGGACACAGGTCAG-TTGTAT. pSUPER-GFP was a gift from S. Nijman (NKI) and pBS(SK-)-Daxin-myc from R. Nusse (Stanford). For *X. laevis* injection studies we used HA-ß-catenin (Funayama et al., 1995), ß-galactosidase in pCS2+ (gift from R. Rupp, Munich). pCS2+MT-RanBP3 t and "wv" mutant were constructed by inserting PCR fragments into the EcoRI and XbaI sites of pCS+Myc. mRFP-ΔGSK3 ß-catenin was constructed by inserting a BamHI/SacII digested PCR fragment spanning the ORF derived from pRK5–SK-catenin-GSK (R. Nusse) into the BglII and SacII sites of mRFP (Campbell et al., 2002).

Cell culture, transfection and reporter assays
Cells were cultured in DMEM or in RPMI (NCI-H28), supplemented with 10% fetal calf serum, penicillin/streptomycin (Gibco-BRL) and were transfected using Fugene-6 (Roche) as instructed by the supplier. For reporter assays, cells were cultured in 12 wells plates and transfected with 100 ng TOP/FOP-Tk-luc, 0.5 ng pRL-CMV, 10 ng Wnt1, 30 ng GFP-ß-catenin, 20 (HEK293) or 100 (NCI-H28) ng ΔGSK3-ß-catenin, 100 ng GFP-CRM1 and 100 ng RanBP3 wt/mutant or as indicated. Luciferase activity was measured 48 hrs post transfection using the Dual-Luciferase Reporter Assay System (Promega). Reporter assays using shRNAs were performed as above using 200 ng shRNA constructs and luciferase activity was measured 72 hrs after transfection. HCT116 cells were grown to 50% confluency in 10 cm dishes and transfected with 5 µg of either ß-Galactosidase, RanBP3 wt or wv mutant expression constructs and 0.5 µg EGFP-N3 plasmid to select for transfected cells. 40 hrs after transfection, GFP-positive cells were collected using flow cytometry. Cells were lysed in sample buffer and 200,000 cells were resolved on a 10% SDS-PAGE gel and analyzed by Western blotting.

Protein expression and purification
GST, GST-ARM (amino acids 144-665) and GST-ß-catenin (Wiechens and Fagotto, 2001) were expressed in E. coli strain BL21-pLysS and lysed by sonification in 500 mM NaCl; 20 mM Hepes-KOH pH 7.9; 8.7% glycerol; 2.5 mM 2-Mercaptoethanol supplemented with protease inhibitors (Complete protease inhibitor cocktail tablets, Roche). GST-ß-catenin fusion proteins were purified from post ribosomal supernatants using Protein G Sepharose (Amersham Biosciences). His-tagged Ran RanQ69L, RanBP1 and RanGAP were expressed as previously described (Englmeier et al., 2001; Izaurralde et al., 1997). 6x His-tagged RanBP3a/b wt and "wv" mutant proteins were gifts from Drs. L. Englmeier and I. Mattaj (EMBL, Heidelberg, Germany).

Western blotting
Proteins were analyzed by SDS-polyacrylamide gel electrophoresis (25 µg per lane) and Western blotting using Immobilon-P transfer membrane (Millipore). Aspecific sites were blocked with 5% non-fat milk at RT for one hour. Primary antibodies were incubated in 1% non-fat milk overnight at 4°C or 1-3 hours at RT in the following dilutions: ß-catenin C19220 1:5000, ABC 1:500; RanBP3 1:5000, TCF4 1:500; 414 1:1:1000; Tubulin 1:20; Actin 1:5000; C-Myc 1:1000. Blots were washed with phosphate buffered saline (PBS)/0.05% Tween 20. Enhanced chemiluminescence (Amersham) was used for detection of proteins.

Immunofluorescence and confocal microscopy

SW480 and DLD1 cells were transfected with 600 ng RanBP3 per 6 well using Fugene 6 (Roche). 45 hrs after transfection cells were either fixed for 10 min in 3.7% formaldehyde in PBS, permeabilized for 5 min in 0.2% Triton/PBS and incubated for one hour at room temperature with primary antibodies diluted in 0.05% BSA/PBS. Cells were washed in PBS and incubated in fluorescently conjugated secondary antibody (Molecular Probes) and mounted in Vectashield (Vector Laboratories). Images were recorded using a Leica NT confocal microscope. Hek 293 cells were transfected with 40 ng mRFP-GSK3-ß-catenin, 200 ng RanBP3 and/or 200 ng GFP-Rev-NES per 6 well using Fugene 6. After 40 hrs cells were either treated or not treated with 50 nM LMB for 1 hour. Cells were fixed for 10 min in 3.7% formaldehyde in PBS and mounted in Vectashield. In each condition, cells with equally low expression were recorded with a Leica SP2 TCS AOBS confocal microscope. Nuclear and cytoplasmic regions of confocal images were quantified, background subtracted and nuclear-cytoplasmic ratios were calculated using Image J software.

***In vitro* binding studies**

In pull down assays 750 pmol GST, GST-ß-catenin or GST-ARM were incubated for 1 hr at 4°C with *X. laevis* extracts (Hetzer et al., 2000) 1:1 diluted in 200 mM NaCl, 20 mM Hepes-KOH pH 7.9, 8.7% glycerol, 2.5 mM 2-Mercaptoethanol (Buffer A). RanQ69L was added at 2 µM. In binding assays using HeLa nuclear extracts (obtained from 4C Biotech) RanQ69L was used at 1 µM. Proteins were eluted with buffer A supplemented with 300 mM NaCl. After TCA precipitation, proteins were analyzed by Western blot. Pull down assays using all recombinant proteins were performed by incubating for 1 hr at 4°C; 1.5 µM GST-ß-catenin beads with 0.2, 0.5 or 2 µM wt or "wv" mutant RanBP3 and 2 µM Ran-GTP in PBS, 8.7% glycerol, 2 mM $MgCl_2$. Proteins were eluted with 500 mM NaCl, 8.7% glycerol, 2 mM $MgCl_2$, 2.5 mM 2-Mercaptoethanol in the presence or absence of RanBP1 or RanGAP in PBS, and prepared for analysis on SDS-PAGE.

Cell fractionation

For cell fractionation we used the protocol of Andrews and Faller (1991) with the following adaptations: Cells and nuclei were spun down at 4°C for 3 min at 500 and 300 g respectively. 10 mM NaF, 2 mM $NaVO_3$ and protease inhibitors (Complete protease inhibitor cocktail tablets minus EDTA, Roche) were added to the lysis buffers. After incubation in hypotonic buffer, NP-40 was added to a concentration of 10%, samples were vortexed shortly and passed through a 25G needle. Whole cell extracts were reconstituted by mixing nuclear and cytosol extracts.

***X. laevis* injection studies**

mRNAs were synthesized *in vitro* using SP6 polymerase (Promega). mRNAs were injected in the subequatorial region of a dorsal or ventral blastomere at the 4-cell stage as described previously (Fagotto et al., 1996; Fagotto et al., 1997). Embryos were raised in 0.1x MBSH (88 mM NaCl, 1 mM KCl, 2.4 mM $NaHCO_3$, 0.82 mM $MgSO_4$, 0.33 mM $Ca(NO_3)_2$, 0.41 mM $CaCl_2$, 10 mM HEPES, pH 7.4, 10 mg/ml benzylpenicillin, 10 mg/ml streptomycin) until tail bud stage and scored. RNA was prepared from late stage 9 embryos as previously described (Schohl and Fagotto, 2003).

dsRNA synthesis *D. melanogaster*

ß-galactosidase, Daxin and RanBP3 dsRNAs were synthesized according to Kennerdel and Carthew (1998) and purified using S400 Spin Columns (Pharmacia). PCR products were verified by DNA sequencing. For *D. melanogaster* RanBP3 dsRNA, two 750 bps fragments that span exon-2 of the *D. melanogaster* RanBP3 gene (GC10225) were amplified from genomic DNA. Fragment 1 spans the RanBP3 open reading frame (ORF) from position 341-1104, fragment 2 from position 683 to 3'UTR position 1423. The following primers were used: BP3 sense primer-1: AGAACAACATGCCAAATGTTCAG; BP3 anti sense primer-1: GACGCCG-TTTTTCGCTTCCTCT; BP3 sense primer-2: AGAAACGCAAATACGAGGAGGT; BP3 anti sense primer-2: GGCGCGCTTTATTAATTAGTGT. pBS(SK-)-Daxin-myc (Willert et al., 1999) was used as a template to generate a 750 bps dsRNA Daxin fragment spanning nucleotides 1462-2210. Daxin sense primer: GAGAAGTTTGCACTGGACGAAGA and Daxin antisense primer: GGCTTGACAAGACCCATCGCTT. For ß-gal dsRNA, nucleotides spanning 1296 to 1921 of the lac operon (NCBI accession # J01636.) were sub-cloned into pGEMT-easy and T7 RNA polymerase promoters were added by PCR of the linearized plasmid.

Cuticle analysis and immuno histochemistry

Embryos were prepared for injections as previously described (Kennerdell and Carthew, 1998) with minor modifications. Embryos were injected with 3 µM dsRNA and for RanBP3 RNAi, an 1:1 mixture of two dsRNA fragments was used. After

injection, the embryos were covered with oil and incubated for 48 hrs at 18°C in a humified chamber. After incubation, the embryos were manually dissected from their viteline membranes and incubated overnight at 65°C in glycerol/acetic acid (1:3). The next day, embryos were mounted in Hoyers mounting medium and incubated for 1-2 days at 55°C and visualized by dark field microscopy. For anti-Engrailed antibody staining, embryos were incubated for 15 hrs, fixed, manually devitalinized and processed for antibody staining according to standard procedures (Patel, 1994).

D. melanogaster RT-PCR

Dechorionated wild type embryos were injected with buffer or RanBP3 dsRNA and then aged at 16 degrees for 15 hours. RNA was prepared and treated with DNAse (RNA-Easy kit, Qiagen) and randomly primed first-strand cDNA was prepared using SuperScript kit (InVitrogen), both according to the manufacturers protocol. Samples for the RP49-specific control PCRs were initially diluted 80-fold to compensate for higher expression levels. Subsequently, a series of 2-fold dilutions was performed for each sample; one µl of each dilution was used in a PCR reaction. Primers were chosen to span an intron to allow discrimination of PCR products originating from contaminating genomic DNA from those originating from first-strand cDNA. Primers used were as follows: RanBP3 Forward (AGTGACAGCGATAACACAGCGATAA), RanBP3 Reverse (GCAGAAACG-GATTATTCAGCAGG), RP49 Forward (ATGACCATCCGCCCAGCA) and RP49 Reverse (TTGGGGTTGGTGAG-GCGGAC). 30-cycle PCRs were performed using SuperTaq Plus polymerase (SpheroQ) and equal volumes of the reaction products were electrophoresed on 1.5% agarose gels and visualized by ethidium bromide staining.

Acknowledgements

We thank Lee Fradkin and Monique Radjkoemar-Bansraj for designing and performing RT-PCR, Bernike Kalverda for literature analysis of the 19p13.3 region, Hans Clevers, Robert Kypta, Iain Mattaj, Roel Nusse and Renee van Amerongen for providing reagents, Reuven Agami for pSUPER plasmid, Lauran Oomen and Lenny Brocks for valuable assistance in confocal microscopy and Frank van Diepen and Anita Pfauth for help with flow cytometry, Helen Pickersgill for experimental advice, and all Fornerod lab members for helpful discussions and critically reading the manuscript. J.H. is supported by grants from The Netherlands Science Foundation Medical Sciences and the Dutch Cancer Foundation NKB/KWF.

Abbreviations list

Abbreviations used in this paper: APC, adenomatous polyposis coli; GSK3ß, glycogen synthase kinase 3ß; RNAi, RNA interference; shRNA, short hairpin RNA; dsRNA, double stranded RNA, NES, nuclear export signal

References

Andrews, N.C., and D.V. Faller. 1991. A rapid micropreparation technique for extraction of DNA-binding proteins from limiting numbers of mammalian cells. Nucleic Acids Res. 19:2499.

Barker, N., A. Hurlstone, H. Musisi, A. Miles, M. Bienz, and H. Clevers. 2001. The chromatin remodelling factor Brg-1 interacts with beta-catenin to promote target gene activation. Embo J. 20:4935-43.

Behrens, J., B.A. Jerchow, M. Wurtele, J. Grimm, C. Asbrand, R. Wirtz, M. Kuhl, D. Wedlich, and W. Birchmeier. 1998. Functional interaction of an axin homolog, conductin, with beta-catenin, APC, and GSK3beta. Science. 280:596-9.

Behrens, J., J.P. von Kries, M. Kuhl, L. Bruhn, D. Wedlich, R. Grosschedl, and W. Birchmeier. 1996. Functional interaction of beta-catenin with the transcription factor LEF-1. Nature. 382:638-42.

Bienz, M., and H. Clevers. 2000. Linking colorectal cancer to Wnt signaling. Cell. 103:311-20.
Boutros, M., and M. Mlodzik. 1999. Dishevelled: at the crossroads of divergent intracellular signaling pathways. Mech Dev. 83:27-37.

Brannon M, Gomperts M, Sumoy L, Moon RT, Kimelman D. 1997. A beta-catenin/XTcf-3 complex binds to the siamois promoter to regulate dorsal axis specification in Xenopus. Genes Dev. 11:2359-70.

Brannon, M., J.D. Brown, R. Bates, D. Kimelman, and R.T. Moon. 1999. XCtBP is a XTcf-3 co-repressor with roles throughout Xenopus development. Development. 126:3159-70.

Brummelkamp, T.R., R. Bernards, and R. Agami. 2002. A system for stable expression of short interfering RNAs in mammalian cells. Science. 296:550-3.

Calvo, R., J. West, W. Franklin, P. Erickson, P. Bemis, E. Li, B. Helfrich, P. Bunn, J. Roche, E. Brambilla, R. Rosell, R.M. Gemmill, and H.A. Drabkin. 2000. Altered HOX and WNT7A expression in human lung cancer. Proc Natl Acad Sci USA 97: 12776–12781.

Campbell, R.E., O. Tour, A.E. Palmer, P.A. Steinbach,

G.S. Baird, D.A. Zacharias, and R.Y. Tsien. 2002. A monomeric red fluorescent protein. Proc Natl Acad Sci U S A. 99:7877-82.

Cavallo, R.A., R.T. Cox, M.M. Moline, J. Roose, G.A. Polevoy, H. Clevers, M. Peifer, and A. Bejsovec. 1998. Drosophila Tcf and Groucho interact to repress Wingless signaling activity. Nature. 395:604-8.

Chen, G., J. Fernandez, S. Mische, and A.J. Courey. 1999. A functional interaction between the histone deacetylase Rpd3 and the corepressor groucho in Drosophila development. Genes Dev. 13:2218-30.

Dexter, D.L., J.A. Barbosa, and P. Calabresi. 1979. N,N-dimethylformamide-induced alteration of cell culture characteristics and loss of tumorigenicity in cultured human colon carcinoma cells. Cancer Res. 39:1020-5.

Dundr, M., J.G. McNally, J. Cohen, and T. Misteli. 2002. Quantitation of GFP-fusion proteins in single living cells. J Struct Biol. 140:92-9.

Eleftheriou, A., M. Yoshida, and B.R. Henderson. 2001. Nuclear export of human beta-catenin can occur independent of CRM1 and the adenomatous polyposis coli tumor suppressor. J Biol Chem. 276:25883-8.

Englmeier, L., M. Fornerod, F.R. Bischoff, C. Petosa, I.W. Mattaj, and U. Kutay. 2001. RanBP3 influences interactions between CRM1 and its nuclear protein export substrates. EMBO Rep. 2:926-32.

Fagotto, F., N. Funayama, U. Gluck, and B.M. Gumbiner. 1996. Binding to cadherins antagonizes the signaling activity of beta-catenin during axis formation in Xenopus. J Cell Biol. 132:1105-14.

Fagotto, F., K. Guger, and B.M. Gumbiner. 1997. Induction of the primary dorsalizing center in Xenopus by the Wnt/GSK/beta-catenin signaling pathway, but not by Vg1, Activin or Noggin. Development. 124:453-60.

Funayama, N., F. Fagotto, P. McCrea, and B.M. Gumbiner. 1995. Embryonic axis induction by the armadillo repeat domain of beta-catenin: evidence for intracellular signaling. J Cell Biol. 128:959-68.

Giannini, A.L., M.M. Vivanco, and R.M. Kypta. 2000. Analysis of beta-catenin aggregation and localization using GFP fusion proteins: nuclear import of alpha-catenin by the beta-catenin/Tcf complex. Exp Cell Res. 255:207-20.

Groden, J., A. Thliveris, W. Samowitz, M. Carlson, L. Gelbert, H. Albertsen, G. Joslyn, J. Stevens, L. Spirio, M. Robertson, and et al. 1991. Identification and characterization of the familial adenomatous polyposis coli gene. Cell. 66:589-600.

Hart, M.J., R. de los Santos, I.N. Albert, B. Rubinfeld, and P. Polakis. 1998. Downregulation of beta-catenin by human Axin and its association with the APC tumor suppressor, beta-catenin and GSK3 beta. Curr Biol. 8:573-81.

He, X., J.P. Saint-Jeannet, J.R. Woodgett, H.E. Varmus, and I.B. Dawid. 1995. Glycogen synthase kinase-3 and dorsoventral patterning in Xenopus embryos. Nature. 374:617-22.

He, T.C., A.B. Sparks, C. Rago, H. Hermeking, L. Zawel, L.T. da Costa, P.J. Morin, B. Vogelstein, and K.W. Kinzler. 1998. Identification of c-MYC as a target of the APC pathway. Science 281:1509-12.

Hecht, A., and R. Kemler. 2000. Curbing the nuclear activities of beta-catenin. Control over Wnt target gene expression. EMBO Rep. 1:24-8.

Henderson, B.R. 2000. Nuclear-cytoplasmic shuttling of APC regulates beta-catenin subcellular localization and turnover. Nat Cell Biol. 2:653-60.

Henderson, B.R., and A. Eleftheriou. 2000. A comparison of the activity, sequence specificity, and CRM1-dependence of different nuclear export signals. Exp Cell Res. 256:213-24.

Henderson, B.R., and F. Fagotto. 2002. The ins and outs of APC and beta-catenin nuclear transport. EMBO Rep. 3:834-9.

Hetzer, M., D. Bilbao-Cortes, T.C. Walther, O.J. Gruss, and I.W. Mattaj. 2000. GTP hydrolysis by Ran is required for nuclear envelope assembly. Mol Cell. 5:1013-24.

Ikeda, S., S. Kishida, H. Yamamoto, H. Murai, S. Koyama, and A. Kikuchi. 1998. Axin, a negative regulator of the Wnt signaling pathway, forms a complex with GSK-3beta and beta-catenin and promotes GSK-3beta-dependent phosphorylation of beta-catenin. Embo J. 17:1371-84.

Itoh, K., V.E. Krupnik, and S.Y. Sokol. 1998. Axis determination in Xenopus involves biochemical interactions of axin, glycogen synthase kinase 3 and beta-catenin. Curr Biol. 8:591-4.

Izaurralde, E., U. Kutay, C. von Kobbe, I.W. Mattaj, and D. Gorlich. 1997. The asymmetric distribution of the constituents of the Ran system is essential for transport into and out of the nucleus. EMBO J. 16:6535-47.

Kao, K. R. and Elinson, R. P. 1988. The entire mesodermal mantle behaves as Spemann's organizer in dorsoanterior enhanced Xenopus laevis embryos. Dev. Biol. 127:64-77.

Kato, N., M. Romero, L. Catasus, and J. Prat. 2004. The STK11/LKB1 Peutz-Jegher gene is not involved in the pathogenesis of sporadic sex cord-stromal tumors, although loss of heterozygosity at 19p13.3 indicates other gene alteration in these tumors. Hum Pathol. 35:1101-4.

Kennerdell, J.R., and R.W. Carthew. 1998. Use of dsRNA-mediated genetic interference to demonstrate that frizzled and frizzled 2 act in the wingless pathway. Cell. 95:1017-26.

Kinzler, K.W., M.C. Nilbert, L.K. Su, B. Vogelstein, T.M. Bryan, D.B. Levy, K.J. Smith, A.C. Preisinger, P. Hedge, D. McKechnie, and et al. 1991. Identification of FAP locus genes from chromosome 5q21. Science. 253:661-5.

Korinek, V., N. Barker, P.J. Morin, D. van Wichen, R. de Weger, K.W. Kinzler, B. Vogelstein, and H. Clevers. 1997. Constitutive transcriptional activation by a beta-catenin-Tcf complex in APC-/- colon carcinoma. Science. 275:1784-7.

Kramps, T., O. Peter, E. Brunner, D. Nellen, B. Froesch, S. Chatterjee, M. Murone, S. Zullig, and K. Basler. 2002. Wnt/wingless signaling requires BCL9/legless-mediated recruitment of pygopus to the nuclear beta-catenin-TCF complex. Cell. 109:47-60.

Lee, J.Y., S.M. Dong, H.S. Kim, S.Y. Kim, E.Y. Na, M.S. Shin, S.H. Lee, W.S. Park, K.M. Kim, Y.S. Lee, J.J. Jang, and N.J. Yoo. 1998. A distinct region of chromosome 19p13.3 associated with the sporadic form of adenoma malignum of the uterine cervix. Cancer Res. 58:1140-3.

Levanon, D., R.E. Goldstein, Y. Bernstein, H. Tang, D. Goldenberg, S. Stifani, Z. Paroush, and Y. Groner. 1998. Transcriptional repression by AML1 and LEF-1 is mediated by the TLE/Groucho corepressors. Proc Natl Acad Sci U S A. 95:11590-5.

Lindsay, M.E., J.M. Holaska, K. Welch, B.M. Paschal, and I.G. Macara. 2001. Ran-binding protein 3 is a cofactor for Crm1-mediated nuclear protein export. J Cell Biol. 153:1391-402.

Mao, J., J. Wang, B. Liu, W. Pan, G.H. Farr, 3rd, C. Flynn, H. Yuan, S. Takada, D. Kimelman, L. Li, and D. Wu. 2001. Low-density lipoprotein receptor-related protein-5 binds to Axin and regulates the canonical Wnt signaling pathway. Mol Cell. 7:801-9.

Miyai, K., Y. Furugen, T. Matsumoto, K. Iwabuchi, S. Hirose, K. Kinoshita, and H. Fujii. 2004. Loss of heterozygosity analysis in uterine cervical adenocarcinoma. Gynecol Oncol. 94:115-20.

Molenaar, M., M. van de Wetering, M. Oosterwegel, J. Peterson-Maduro, S. Godsave, V. Korinek, J. Roose, O. Destree, and H. Clevers. 1996. XTcf-3 transcription factor mediates beta-catenin-induced axis formation in Xenopus embryos. Cell. 86:391-9.

Mueller, L., V.C. Cordes, F.R. Bischoff, and H. Ponstingl. 1998. Human RanBP3, a group of nuclear RanGTP binding proteins. FEBS Lett. 427:330-6.

Neufeld, K.L., F. Zhang, B.R. Cullen, and R.L. White. 2000. APC-mediated downregulation of beta-catenin activity involves nuclear sequestration and nuclear export. EMBO Rep. 1:519-23.

Noguchi, E., Y. Saitoh, S. Sazer, and T. Nishimoto. 1999. Disruption of the YRB2 gene retards nuclear protein export, causing a profound mitotic delay, and can be rescued by overexpression of XPO1/CRM1. J Biochem (Tokyo). 125:574-85.

Noordermeer, J., P. Johnston, F. Rijsewijk, R. Nusse, and P.A. Lawrence. 1992. The consequences of ubiquitous expression of the wingless gene in the Drosophila embryo. Development. 116:711-9.

Nusse, R. 1999. WNT targets. Repression and activation. Trends Genet. 15:1-3.

Nusslein-Volhard, C., and E. Wieschaus. 1980. Mutations affecting segment number and polarity in Drosophila. Nature. 287:795-801.

Oesterreich, S., D.C. Allredl, S.K. Mohsin, Q. Zhang, H. Wong, A.V. Lee, C.K. Osborne, and P. O'Connell. 2001. High rates of loss of heterozygosity on chromosome 19p13 in human breast cancer. Br J Cancer. 84:493-8.

Parker, D.S., J. Jemison, and K.M. Cadigan. 2002. Pygopus, a nuclear PHD-finger protein required for Wingless signaling in Drosophila. Development. 129:2565-76.

Patel, N.H. 1994. Imaging neuronal subsets and other cell types in whole-mount Drosophila embryos and larvae using antibody probes. Methods Cell Biol. 44:445-87.

Patel, N.H., E. Martin-Blanco, K.G. Coleman, S.J. Poole, M.C. Ellis, T.B. Kornberg, and C.S. Goodman. 1989. Expression of engrailed proteins in arthropods, annelids, and chordates. Cell. 58:955-68.

Phair, R.D., S.A. Gorski, and T. Misteli. 2004. Measurement of dynamic protein binding to chromatin *in vivo*, using photobleaching microscopy. Methods Enzymol. 375:393-414.

Polakis, P. 2000. Wnt signaling and cancer. Genes Dev. 14:1837-51.

Quinn, L.A., G.E. Moore, R.T. Morgan, and L.K. Woods. 1979. Cell lines from human colon carcinoma with unusual cell products, double minutes, and homogeneously staining regions. Cancer Res. 39:4914-24.

R Development Core Team (2005). R: A language and environment for statistical computing. R Foundation for Statistical Computing, Vienna, Austria. ISBN 3-900051-07-0, URL http://www.R-project.org.

Roose, J., M. Molenaar, J. Peterson, J. Hurenkamp, H. Brantjes, P. Moerer, M. van de Wetering, O. Destree, and H. Clevers. 1998. The Xenopus Wnt effector XTcf-3 interacts with Groucho-related transcriptional repressors. Nature. 395:608-12.

Rosin-Arbesfeld, R., A. Cliffe, T. Brabletz, and M. Bienz. 2003. Nuclear export of the APC tumour suppressor controls beta-catenin function in transcription. Embo J. 22:1101-13.

Rosin-Arbesfeld, R., F. Townsley, and M. Bienz. 2000. The APC tumour suppressor has a nuclear export func-

tion. Nature. 406:1009-12.

Sakanaka, C., J.B. Weiss, and L.T. Williams. 1998. Bridging of beta-catenin and glycogen synthase kinase-3beta by axin and inhibition of beta-catenin-mediated transcription. Proc Natl Acad Sci U S A. 95:3020-3.

Schohl, A, and F. Fagotto. 2003. A role for maternal beta-catenin in early mesoderm induction in Xenopus. EMBO J. 22:3303-13.

Staal, F.J., M. Noort Mv, G.J. Strous, and H.C. Clevers. 2002. Wnt signals are transmitted through N-terminally dephosphorylated beta-catenin. EMBO Rep. 3:63-8.

Tago, K., T. Nakamura, M. Nishita, J. Hyodo, S. Nagai, Y. Murata, S. Adachi, S. Ohwada, Y. Morishita, H. Shibuya, and T. Akiyama. 2000. Inhibition of Wnt signaling by ICAT, a novel beta-catenin-interacting protein. Genes Dev. 14:1741-9.
Takemaru, K., S. Yamaguchi, Y.S. Lee, Y. Zhang, R.W. Carthew, and R.T. Moon. 2003. Chibby, a nuclear beta-catenin-associated antagonist of the Wnt/Wingless pathway. Nature. 422:905-9.

Takemaru, K.I., and R.T. Moon. 2000. The transcriptional coactivator CBP interacts with beta-catenin to activate gene expression. J Cell Biol. 149:249-54.

Taura, T., H. Krebber, and P.A. Silver. 1998. A member of the Ran-binding protein family, Yrb2p, is involved in nuclear protein export. Proc Natl Acad Sci U S A. 95:7427-32.

Thompson, B., F. Townsley, R. Rosin-Arbesfeld, H. Musisi, and M. Bienz. 2002. A new nuclear component of the Wnt signaling pathway. Nat Cell Biol. 4:367-73.

Tolwinski, N.S., M. Wehrli, A. Rives, N. Erdeniz, S. DiNardo, and E. Wieschaus. 2003. Wg/Wnt signal can be transmitted through arrow/LRP5,6 and Axin independently of Zw3/Gsk3beta activity. Dev Cell. 4:407-18.

Tucci, S., W. Futterweit, E.S. Concepcion, D.A. Greenberg, R. Villanueva, T.F. Davies, and Y. Tomer. 2001. Evidence for association of polycystic ovary syndrome in caucasian women with a marker at the insulin receptor gene locus. J Clin Endocrinol Metab. 86:446-9.

van Es, J.H., C. Kirkpatrick, M. van de Wetering, M. Molenaar, A. Miles, J. Kuipers, O. Destree, M. Peifer, and H. Clevers. 1999. Identification of APC2, a homologue of the adenomatous polyposis coli tumour suppressor. Curr Biol. 9:105-8.

van Noort, M., J. Meeldijk, R. van der Zee, O. Destree, and H. Clevers. 2002. Wnt signaling controls the phosphorylation status of beta-catenin. J Biol Chem. 277:17901-5.

Waltzer, L., and M. Bienz. 1998. Drosophila CBP represses the transcription factor TCF to antagonize Wingless signaling. Nature. 395:521-5.

Wharton, K.A., Jr. 2003. Runnin' with the Dvl: proteins that associate with Dsh/Dvl and their significance to Wnt signal transduction. Dev Biol. 253:1-17.

Wiechens, N., and F. Fagotto. 2001. CRM1- and Ran-independent nuclear export of beta-catenin. Curr Biol. 11:18-27.

Willert, K., C.Y. Logan, A. Arora, M. Fish, and R. Nusse. 1999. A Drosophila Axin homolog, Daxin, inhibits Wnt signaling. Development. 126:4165-73.

Wolff, B., J.J. Sanglier, and Y. Wang. 1997. Leptomycin B is an inhibitor of nuclear export: inhibition of nucleocytoplasmic translocation of the human immunodeficiency virus type 1 (HIV-1) Rev protein and Rev-dependent mRNA. Chem Biol. 4:139-47.

Yanaihara, N., A. Okamoto, and S. Matsufuji. 2003. A commonly deleted region in ovarian cancer on chromosome 19p13.3, not including the OAZ1 gene. Int J Oncol. 23:567-75.

Yang, T.L., Y.R. Su, C.S. Huang, J.C. Yu, Y.L. Lo, P.E. Wu, and C.Y. Shen. 2004. High-resolution 19p13.2-13.3 allelotyping of breast carcinomas demonstrates frequent loss of heterozygosity. Genes Chromosomes Cancer. 41:250-6.

Zeng, L., F. Fagotto, T. Zhang, W. Hsu, T.J. Vasicek, W.L. Perry, 3rd, J.J. Lee, S.M. Tilghman, B.M. Gumbiner, and F. Costantini. 1997. The mouse Fused locus encodes Axin, an inhibitor of the Wnt signaling pathway that regulates embryonic axis formation. Cell. 90:181-92.